IEEE Access
Multidisciplinary | Rapid Review | Open Access Journal

Received 8 May 2023, accepted 31 May 2023, date of publication 12 June 2023, date of current version 16 June 2023.

Digital Object Identifier 10.1109/ACCESS.2023.3285413

RESEARCH ARTICLE

Gas Losses in Transformers–Influences and Consideration

CHRISTOF RIEDMANN[1], UWE SCHICHLER[1], (Member, IEEE), WOLFGANG HÄUSLER[2], AND WOLFGANG NEUHOLD[2]

[1]Institute of High Voltage Engineering and System Performance, Graz University of Technology, 8010 Graz, Austria
[2]Industrie Automation Graz, Ing. W. Häusler GmbH, 8074 Raaba, Austria

Corresponding author: Christof Riedmann (christof.riedmann@tugraz.at)

This work was supported in part by the "Österreichische Forschungsförderungsgesellschaft (FFG)" under Grant 874800, and in part by the Graz University of Technology (TU Graz) Open Access Publishing Fund.

ABSTRACT Dissolved gas analysis (DGA) is frequently used for the condition assessment and monitoring of transformers. In the case of free-breathing transformers, gas losses may occur at the phase interface due to the chaotic molecular movement of the dissolved gas molecules. These gas losses and the resulting distortion of the interpretation basis for the DGA can lead to a false assessment of the condition. Furthermore, the relative ratios may shift, which in turn can lead to the misclassification of the present defect. This paper deals with the influences on gas losses and describes a possible consideration for use in the condition assessment. It begins with an explanation of the gas losses problem in more detail based on theoretical considerations and summarised in hypotheses. In addition to the experimental methods used, theoretical model considerations for taking gas losses into account are described below. The results deal on the one hand with the influences on the gas losses (geometry and temperature) and the other hand with the application of the developed model for the consideration of the gas losses. In detail, the results of the gassing behaviour of different complex geometries – simple phase interfaces, a transformer model and a distribution transformer – are described in more detail and it is shown that a correction of the degassing with the model is possible within certain limits. Furthermore, the methodologies for determining the model are discussed in this paper.

INDEX TERMS Transformer, dissolved gas analysis, gas losses, gas management, molecular movement.

I. INTRODUCTION

Dissolved gas analysis (DGA) is one of the most commonly used method for assessing and monitoring the condition of transformers. Energy introduced into the transformer by electrical and/or thermal stress can cause the binding energy of the insulating material molecules to be exceeded. The bonds break and the resulting unstable decomposition products recombine to form gaseous molecules [1].

Every closed physical system strives towards a state of equilibrium. After a defect occurs, the gases are initially concentrated at the defect location. Subsequently, a state of equilibrium is reached by diffusion. This process is accelerated by internal oil flows [2], [3].

The associate editor coordinating the review of this manuscript and approving it for publication was Norhafiz Azis.

In free-breathing transformers, the gas space in the conservator tank, as well as the ambient air, must also be considered as part of the overall system (Fig. 1). Most of the key gases used in DGA are not present in any significant concentration in the ambient air. Thus, gas molecules diffuse from the insulating liquid into the ambient air. In addition, air gases are dissolved in the insulating liquid. These changes in the gas concentrations and resulting relative ratios of the gas concentrations to each other can influence the dissolved gas analysis [1], [2], [4].

II. DGA FOR FREE-BREATHING AND HERMETICALLY SEALED TRANSFORMERS

A. CONDITION ASSESSMENT

In the case of free-breathing transformers, the ambient air determines the targeted state. For most hydrocarbons, this

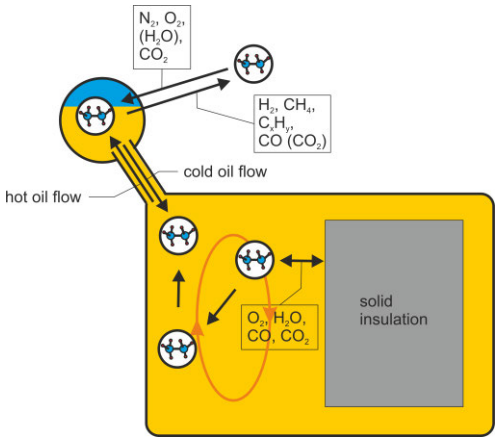

FIGURE 1. Molecular movements in a free-breathing transformer.

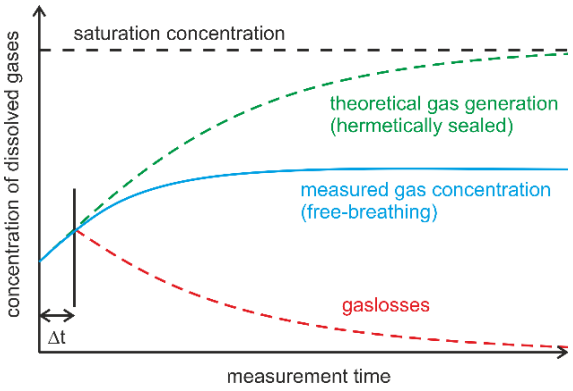

FIGURE 2. Schematic connection between gas formation, gas losses and measured gas concentrations [7].

is zero or, in the case of methane, around 1.89 ppm in the air [5]. The concentration of H_2 and CO in the ambient air is also very low. In contrast, O_2 (20.9% of the air), N_2 (78.1% of the air) and CO_2 (413 ppm of the air) are dissolved in the oil [5], [6].

If an active defect is assumed, gas is generated continuously and the measurable concentration of dissolved gas increases in the transformer. In a free-breathing transformer, gas loss also takes place simultaneously. Thus, an equilibrium is established in the oil volume between the produced gases and the gas losses (Fig. 2). The measured gas concentrations, therefore, do not reflect the real gas quantities produced by the defect [7].

It should be noted at this point that statistical behaviour does not always apply. Depending on the transformer and its geometry as well as the type and position of the defect, the behaviour may vary. In the worst case, defect veiling can occur. Defect veiling is what occurs when a defect is not detected during (interval) measurements because the gas change is very small due to the simultaneous gas losses, or the gas concentration has dropped so much at the time of sampling that a defect is no longer detectable.

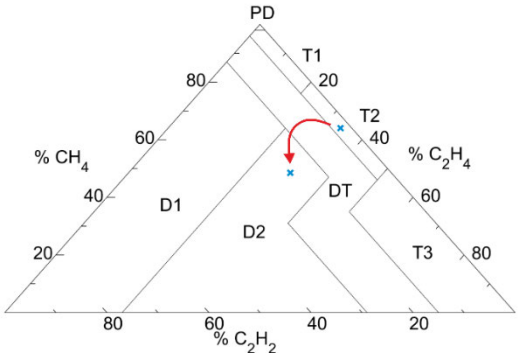

FIGURE 3. Exemplary effects of degassing on duval's triangle 1 [7].

B. DEFECT IDENTIFICATION

Due to the different chemical properties, degassing does not occur with the same velocity for all key gases. Consequently, in addition to the falsification of the condition assessment based on absolute gas concentrations, there may also be a shift in the relative gas ratios. A theoretical case of misinterpretation is shown in Fig. 3, where a thermal defect would be wrongly interpreted as an electrical defect since CH_4 degasses faster than the higher-value hydrocarbons [7].

C. STATEMENTS TO BE ANALYSED

The following essential statements can be derived from the former considerations, which are to be studied and confirmed in the paper.

1) With simultaneous gas formation and gas losses, an equilibrium is established between these processes. The measurable gas concentrations may not reflect the actual defect.
2) Gas losses change the absolute gas concentrations in a transformer, which changes the basis for the condition assessment. In the worst case, the defect may be veiled.
3) Different key gases degas at differing velocities. Due to the resulting shift in relative ratios, the defect type can be misinterpreted.
4) The gas losses and thus the correlations depend on the temperature and the (transformer) geometry.
5) The gas exchange at the phase interface can be taken into account with the aim of a model based on an approach from physical chemistry.

III. METHODOLOGY

A. MEASUREMENT OF GASES AND GAS LOSSES

The partially inhibited naphthenic mineral oil "Nytro 4000A" from Nynas was used for the laboratory tests carried out in the course of this work. To be able to compare the tests with each other, the same starting conditions must be created for each test. Mineral oil which had already been contaminated was not used again. Before each test, the mineral oil was freshly treated in an oil treatment plant.

In the laboratory experiments, a DGA monitoring system was used to monitor the dissolved gases in the test samples. The monitoring system measures six key gases via infrared

spectroscopy, as well as hydrogen and oil moisture via direct measurement in oil. Furthermore, the influence of the monitoring system on degassing was analysed. For this purpose, a test object was equipped with a monitoring system once from the beginning and once after a certain time had elapsed. No difference in the results could be determined.

Different test objects were used for the measurements. Test vessels with a simple phase interface (test objects A, B and C), a transformer model and a distribution transformer were used. The volumes of simple test vessels (A, B and C) are 5.2, 16.3 and 33.9 litres and are filled with 4, 15 and 30 litres of mineral oil. The phase interface extends over 190, 314 and 1350 cm^2 and is always connected to the ambient air via a desiccant air dryer. The transformer model essentially consists of a square main vessel with a connection to a conservator tank in the form of a horizontal cylinder, which in turn is connected to the ambient air via a desiccant air dryer. The main tank has an oil volume of 170 litres. The expansion vessel has a maximum volume of 35 litres, which was half filled. The phase boundary of the transformer model has an area of 1330 cm^2. In addition to these setups, a 0.4/35 kV distribution transformer served as a test object. The transformer has an ONAN cooling. The oil volume of the transformer is 135 litres (filled to half of the conservator tank, phase interface of 1120 cm^2).

B. MODEL FOR TAKING GAS LOSSES INTO ACCOUNT

1) BALANCE EQUATION

The balance equations are the starting point for considerations regarding the gas balance of transformers. Balances always have the same form, are created for a clearly defined balance area and are described with defined limits and boundary conditions. The aim is to specify the storage in the element under consideration as a function of transport flows and conversions [8], [9].

The respective oil volume is considered a clearly defined balance area in the model used. In transformers and other oil-filled equipment, the mass transport flows into the balance volume occur due to the dissolution of gas molecules in the mineral oil. Outgoing mass transport flows are those flows that occur due to the diffusion of gas molecules into the ambient air. The conversion products are those produced by defects. The reversible gas exchange with the solid insulation is currently not taken into account as it is much slower [9]. But, it can be integrated in the same manner as the mass transfer at the interface.

When assessing the condition of transformers, it is not primarily the mass transfer or the change in total mass that are of interest, but rather the concentration c_i of dissolved gas in the mineral oil. In the model developed, the mass transfer across the interface is referred to as the mass flow density $\dot{m}_\mathrm{i}$. Multiplication by time and the expansion area of the boundary layer A_if yields the actual mass flow $\dot{M}_\mathrm{i}$ across the interface. The time here corresponds to the time difference Δt between the two observation times. The equation for determining the concentration $c_{\mathrm{i,k+1}}$ of the $(\mathrm{k+1})^{\mathrm{th}}$ iteration step is given as a function of the previous concentration $c_{\mathrm{i,k}}$ and the current mass flow density $\dot{m}_{\mathrm{i,k}}$ in equation (1). The concentration values are volumetric concentrations. V_oil corresponds to the volume of the mineral oil. Here, ρ_i describes the density of the insulating liquid.

$$c_{i,k+1} = \frac{\left(c_{i,k} \cdot V_{oil} \cdot \rho_i\right) - \left(\dot{m}_{i,k} \cdot A_{if} \cdot \Delta t\right)}{V_{oil} \cdot \rho_i} \tag{1}$$

2) MASS TRANSFER EQUATION

Mass transfer always consists of a combination of a diffusive and a convective component. Often, however, one of the two parts is much smaller than the other and can consequently be neglected [9]. The starting point for the determination of mass transfer in this paper is the boundary layer theory and the surface renewal theory, which can be regarded as special cases of a general theory [10].

In boundary layer theory, it is assumed that a substance is transferred from a solid or stationary liquid surface into a flowing fluid. The concentration drops from $c_{\mathrm{i,if}}$ at the interface to $c_{\mathrm{i},\infty}$ in the bulk (concentration difference Δc_i). The molecule transfer $\dot{n}_\mathrm{i}$ takes place in the area of the thin boundary layer with the thickness δ_i (equation (2)) [9]. D_i corresponds here to the diffusion coefficient and β_i to the mass transfer coefficient.

$$\dot{n}_i = -D_i \frac{\Delta c_i}{\delta_i} = \beta_i \cdot \left(c_{i,if} - c_{i,\infty}\right) \tag{2}$$

In the surface renewal theory, the assumption of laminar boundary layers is abandoned and propagation of turbulence to the interface is assumed. This causes a fluid particle from the bulk to reach the phase interface and the system is thus subject to continuous renewal. At time $t = 0$ s, the particle with a certain mean initial concentration $\bar{c}_\mathrm{i}$ meets the interface with an equilibrium concentration $c_{\mathrm{i,if}}$. During the residence time τ mass transfer occurs by pure diffusion and subsequently the element sinks back into the main mass and mixes with it [9], [11], [12].

For further consideration, the special case of drops is used. The following further assumptions and simplifications are made [8]:

1) Transport occurs from the droplet into the ambient air.
2) At a very great distance, the partial density of the diffusing species is zero.
3) The volume of the droplet is infinitesimal compared to the surroundings.
4) The total diffusion resistance is in the liquid phase.
5) No superimposed flows occur in the respective time horizon.
6) The diameter of the sphere is assumed to be constant in the period under consideration.

For short times t, differential equations can be simplified so that closed solutions can be given. In the above-considered case of a spherical drop with a transient mass transfer, equation (3) results as a solution for short times, assuming that the complete mass transfer resistance is inside the

drop [8].

$$\beta_i = \frac{2}{\sqrt{\pi}} \left(\frac{D_i}{t} \right)^{1/2} \tag{3}$$

The relationships for bubbles and drops apply in principle to any shape, insofar as the object is converted to a fictitious sphere. For this purpose, the object volume V_p is used to determine the equivalent sphere diameter d_e and the equivalent sphere surface A_e [8].

Since the simulation and the real measurements only agree with the drop theory to some extent, special features of the structure must be taken into account in a further step. In contrast to a droplet, the volume is quite large in relation to the exchange area and the path from the ''spherical centre'' to the surface is also quite long. To take this into account, a geometric correction factor K was developed based on the conversion to the ideal drop (equation (4)). h' corresponds to the fictitious distance covered by a molecule between the interface and the centre of the main volume.

$$K = \left(d_e \cdot A_e \cdot \frac{A_{if}}{h'} \right)^2 \tag{4}$$

For the application in more complex geometries, this approach must be extended. The surface renewal theory is used here. The first step for further development is the consideration of the exchange of gas molecules between the main vessel and the conservator tank with a phase interface. It is assumed that the exchange takes only place by oil flows.

With the help of an ultrasonic flow sensor, the flow velocity in the connecting pipe between the conservator tank and the main tank of the distribution transformer was measured. The flow velocity is $u_\mathrm{ex.} = 0.001 - 0.007$ m/s, depending on the temperature. This corresponds to a total oil exchange time of $\tau_\mathrm{rnw} = 11 - 74$ h.

C. MEASUREMENT OF MODEL PARAMETERS

1) HENRY CONSTANTS

Solubility is defined as the amount of a gas that a specific volume of a liquid can absorb under clearly defined conditions. In general, solubility can be described by different coefficients and can be measured by various methods [13], [14], [15], [16], [17], [18], [19].

The mass fraction-related Henry solubility constant $H_\mathrm{i,x}$ used in this work is defined as the partial pressure of gas i in the gas phase p_i to the volumetric mass fraction x_i in the liquid phase at a given temperature T (equation (5)) [20].

$$H_{i,x} = \frac{p_i}{x_i} \tag{5}$$

In principle, there are different ways of measuring solubility coefficients, which are all based on the same principle. This involves bringing a liquid into contact with a gas. Since the dissolved concentration is directly proportional to the partial pressure of the gas (at given boundary conditions), the solubility coefficient can be determined from the dissolved concentration and the partial pressure after a sufficiently long time [13], [15], [16], [21].

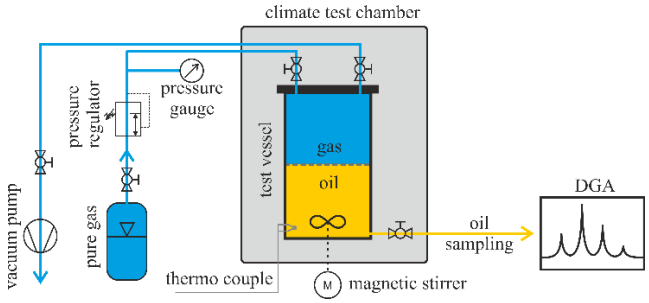

FIGURE 4. Schematic measurement setup for determining the henry constants [1].

Fig. 4 shows the schematic test setup used (based on the principal setup in [13]). The central element of the experimental setup is the test vessel in which the diffusion process takes place. The upper section of the vessel is equipped with connections for the gas supply and a vacuum pump. In the lower area, there is a sampling point and a thermocouple for monitoring the oil temperature. The connections are each equipped with a gas-tight ball valve. The entire setup is placed in a climate test chamber. A magnetic stirrer was integrated into the experimental setup to accelerate the equilibration processes. The concentration of dissolved gases is determined by an external laboratory.

The test object is initially filled with four litres of mineral oil so that there is a residual gas phase of six litres and then degassed further. After 24 hours, the connection to the vacuum pump is closed and the test object is flooded with pure gas. The diffusion process of the gas into the mineral oil begins and is not interrupted until the process stops by itself. After saturation is reached, a manual oil sample is taken according to the test laboratory's instructions and sent to them for analysis. In combination with the recorded pressure, the Henry constant can then be calculated.

2) DIFFUSION COEFFICIENTS

Since calculations as well as the values in the literature for diffusion coefficients of gases in liquids show a very large scattering range that is partly over several orders of magnitude, an empirical approach was chosen in this work [22], [23].

The basic functioning of the diaphragm diffusion cell for empirical determination of the diffusion coefficient in its present form can be traced back to the works of Northrop and Anson as well as McBain and Liu [24], [25]. Two solutions with different initial concentrations are in contact with each other across a membrane. It is assumed that the membrane behaves in the same way as parallel pores. Both solutions are equally distributed in the area of the membrane and mass transfer takes place only by pure diffusion [25], [26]. The diaphragm diffusion cell used to determine the diffusion coefficients is based on that of Stokes [27]. The

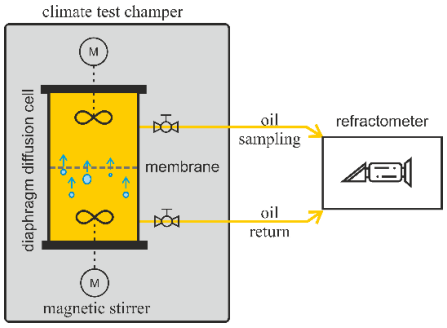

FIGURE 5. Schematic measurement setup for the determination of diffusion coefficients with the diaphragm diffusion cell.

diffusion cell consists of two cylindrical chambers made of aluminium (Fig. 5). The two cylinders are connected by a flange system. The membrane used is a PTFE filter with a thickness of $l_M = 100\ \mu m$ and a pore diameter of $d_P = 1\ \mu m$. Magnetic stirrers are integrated into the two chambers to ensure uniform concentration distribution. The speed of the magnetic stirrers must be constant [27]. In addition, no temperature gradient must occur over time and along the set-up, which is ensured by integrating the entire test set-up into a climate test chamber [26]. It is further essential that the membrane is placed horizontally to avoid internal convection [26; 27]. The denser solution should be placed in the upper chamber for all experiments [27].

Before the measurement, both chambers are filled with the mineral oil and ''conditioned'' for a 24 h period. The initial conditioning ensures that both chambers as well as the membrane pores are filled with mineral oil of the same low concentration at the beginning of the experiments [26]. After conditioning, the oil in the lower chamber of the diaphragm diffusion cell is exchanged with gas-saturated oil.

During the measurement time, molecules from the lower chamber migrated across the membrane into the upper chamber. At the different measuring times, there are different concentration differences between the weaker solution at the top and the stronger solution at the bottom [26]. The diffusion coefficient D can then be determined from these concentration differences according to equation (6) [25], [26]. The concentration differences at the beginning (index 0) and after the time Δt (index f) are determined via the corresponding refractive indices n_i.

$$D = \frac{1}{\Delta t \cdot \beta_{DC}} \cdot \ln \frac{n_{upper,0} - n_{lower,0}}{n_{upper,f} - n_{lower,f}} \tag{6}$$

The cell factor β_{DC} is a geometric constant that results from the structure of the cells and the membrane. Since the determination of the effective pore length and the effective pore diameter is not readily possible, the cell factor is determined experimentally. For the experimental determination, two substances with known diffusion coefficients are used (usually H_2O and NaCl) [27], [28].

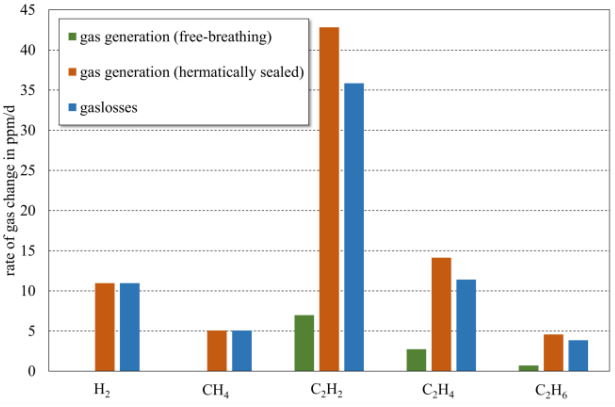

FIGURE 6. Gas formation rates and gas losses in test vessel a during surface discharges.

IV. RESULTS

A. GAS FORMATION RATES OF DIFFERENT DESIGNS

If the same experiment is considered once in the free-breathing configuration and once in the hermetically sealed configuration, clear differences can be seen. In the free-breathing configuration, gas losses occur at the same time as gas formation. The gas losses across the interface can be seen as the difference between the measurements of the two configurations (Fig. 6). The gas formation is significantly greater in the hermetically sealed configuration than in the free-breathing configuration. In the presented experiment, H_2 and CH_4 are not detectable in the free-breathing configuration.

B. EQUILIBRIUM BETWEEN GAS FORMATION AND GAS LOSSES

Fig. 7 shows another test which illustrates the influence of the configuration. During the first 50 hours of operation, the test object was operated with an open connection to the ambient air and then hermetically sealed for approx. 110 hours before the connection to the environment was opened again (gas tight valve in the connection). After a certain detection delay time, the gas concentration first rises continuously after defect activation and then approaches a state of equilibrium between gas formation and gas generation. It should be noted that H_2 is not detectable in this configuration. After the valves to the ambient air are closed, the concentration of dissolved gases increases further if the defect remains unchanged. After a further detection delay time, hydrogen is now also detectable. The dissolved oxygen, which is needed for the production of CO, is consumed and can no longer be dissolved from the environment in the mineral oil – the concentration thus continues to drop. If the connection to the ambient air is opened again after about 160 hours of operation, the concentrations of the generated gases formed drop again to their corresponding state of equilibrium between gas formation and gas losses. New oxygen molecules can now also dissolve, causing the O_2 concentration to rise.

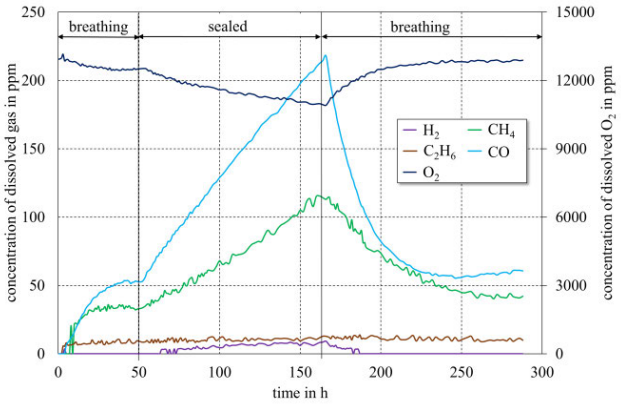

FIGURE 7. Thermal defect in free-breathing and hermetically sealed configuration in test vessel a [7].

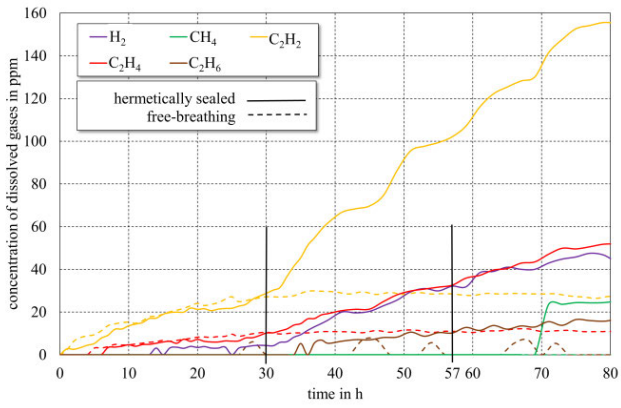

FIGURE 8. Gas formation rates and gas losses in test vessel A during surface discharges.

C. EFFECT OF GAS LOSSES ON CONDITION ASSESSMENT

Fig. 8 shows the difference in gas formation over time between a free-breathing and a hermetically sealed configuration. It can be seen that up to a measuring time of 30 hours, the two configurations behave in the same way. Starting from the defect location, the gas molecules distribute evenly in the mineral oil. From a measuring time of 30 hours, a non-negligible part of the gas molecules reaches the phase interface. In the case of free-breathing configuration, degassing occurs here and an equilibrium is established between gas generation and gas losses. In the case of hermetically sealed operation, no degassing can take place and thus the gas concentrations in the test object continue to rise [7]. It is also particularly striking that less soluble gases such as hydrogen and methane do not reach the detection limit of the measuring system in free-breathing operation.

When analysing the absolute gas concentrations for times > 30 hours, it can be seen that they differ significantly from each other. This also results in different classifications of the condition. If, for example, the condition assessment is considered based on the former IEEE standard (limit values

TABLE 1. Dissolved gas concentration and condition.

Gas		Condition 1	2	3	4
H_2	ppm	<100	<700	<1800	>1800
CH_4	ppm	<120	<400	<1000	>1000
C_2H_2	ppm	<1	<9	<35	>35
C_2H_4	ppm	<50	<100	<200	>200
C_2H_6	ppm	<65	<100	<150	>150
CO	ppm	<350	<570	<1400	>1400
CO_2	ppm	<2500	<4000	<10000	>10000
TDCG	ppm	<720	<1920	<4630	>4630

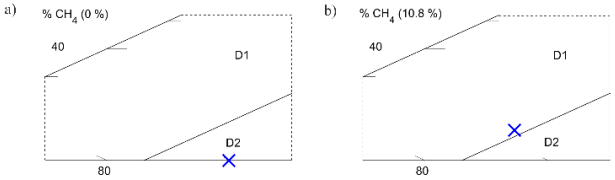

FIGURE 9. Defect classification according to the duval triangle 1 (sections) for test vessel a with surface discharges.

in Table 1), different conditions and recommendations for action results.

The result for hermetically sealed operation from the 32nd hour is the rating "Condition 4" and for free-breathing operation the rating "Condition 3". Depending on the design, different recommendations for action are thus derived from the condition assessment for the same defect. In the case of "Condition 3", transformers are often continued to be operated with reduced load and are taken out of service and maintained in a planned manner. In the case of "Condition 4", the transformer is usually taken out of service directly to avoid consequential damage [1], [29].

If not only the condition but also the defect classification is considered, it can be seen that there is a different classification after 57 hours in the Duval triangle 1. Here, too, different recommendations for action are derived depending on the type of defect. Thus, an electrical discharge with high energy D2 (Fig. 9a) tends to be classified more critically than electrical discharges with low energy D1 (Fig. 9b) at the same gas concentrations.

D. INFLUENCES ON THE GAS LOSSES

In preliminary work by Müller, a linear relationship between the gas losses and the propagation of the phase interface was already established [2]. This is also consistent with the relevant mass transport theories [9].

This effect was exploited in the present work to be able to compare the varying expansions of the phase interface of the individual test vessels. In the following considerations, the

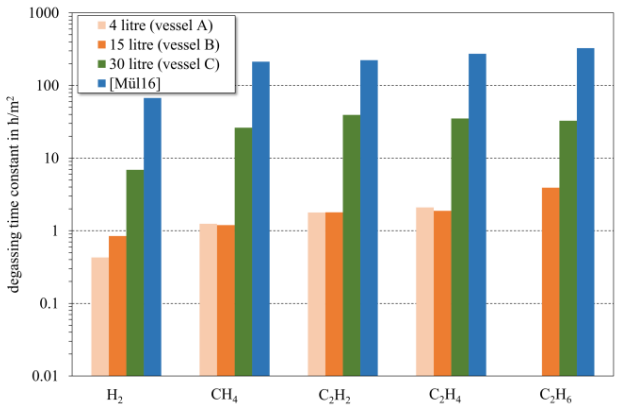

FIGURE 10. Degassing time constants τ_{DG} across simple interfaces.

TABLE 2. Parameters of the time constants as a function of the oil volume for simple interfaces.

	R^2	A_V	B_V
	%	h/m²	1/m³
H_2	96.2	0.23	108.8
CH_4	81.3	0.46	122.5
C_2H_2	82.3	0.66	124.2
C_2H_4	79.7	0.81	113.6
C_2H_6	N/S	0.47	141.3

degassing time constant τ_{DG} is always related to an interface of 1 m² (Fig. 10).

The resulting dependence of the degassing time constant τ_{DG} on the volume V appears to be exponential rather than linear. The corresponding coefficients of determination R^2 as well as the pre-exponential coefficient A_V and the exponential coefficient B_V of equation (7) are given in Table 2. The value of the coefficient of determination for C_2H_6 is not significant due to a lack of data. This approach cannot be directly applied to more complex geometries such as the transformer model (consisting of the main tank, connecting tube and expansion tank) and the real distribution transformer. One possible approach is the surface renewal theory.

$$\tau_{DG}(V) = A_V \cdot e^{B_V \cdot V_{oil}} \tag{7}$$

One of the most important factors influencing the diffusion and gassing behaviour of mineral oil is temperature T_{oil}. Based on the temperature-dependent mobility of the individual molecules, the temperature dependence of the degassing time constants follows. As already stated in literature, the temperature dependence also follows an exponential function [2].

The corresponding coefficients of determination $R^2$and the coefficients A_T and B_T of equation (8) are given in Table 3. The values for C_2H_6 could not be determined correctly.

$$\tau_{DG}(T) = A_T \cdot e^{-B_T \cdot T_{oil}} \tag{8}$$

TABLE 3. Parameters of the time constants as a function of the temperature at the test vessel A.

	R^2	A_T	B_T
	%	h/m²	1/°C
H_2	99.1	0.71	0.022
CH_4	99.1	2.8	0.033
C_2H_2	96.8	4.3	0.034
C_2H_4	96.6	5.5	0.037

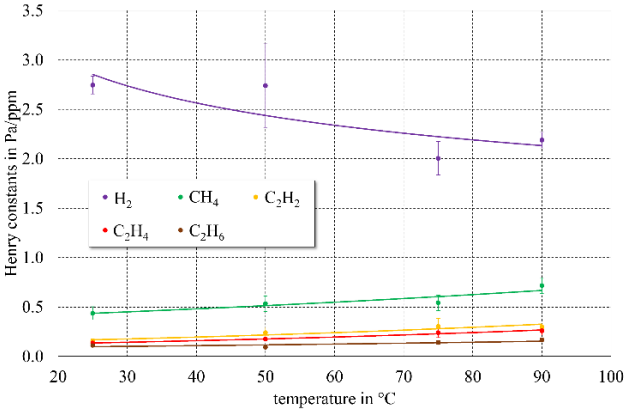

FIGURE 11. Henry constants determined by measurement as a function of temperature.

TABLE 4. Comparison of ostwald coefficients with the literature.

Gas	Ostwald Coefficient			
	Own	[16]	[29]	[13]
H_2	1.17	0.06	0.04	
CH_4	0.82	0.43	0.34	0.38
C_2H_2	1.51	1.24	0.94	0.93
C_2H_4	2.01	1.84	1.35	1.42
C_2H_6	2.61	2.82	1.99	1.8

The exponential constants are similar to those of Müller [2]. However, due to the corresponding geometric conditions, the respective pre-exponential factor A_T depends on the respective test object. Similar to before, different results are also obtained depending on the internal structure or complex geometries.

E. MEASUREMENT OF THE MODEL PARAMETER

1) HENRY CONSTANTS

The Henry constants were investigated for the gases H_2, CH_4, C_2H_2, C_2H_4 and C_2H_6 at temperatures of 25 °C, 50 °C, 75 °C and 90 °C (Fig. 11). After converting the Henry constants into Ostwald coefficients, a comparison with the literature can be made (Tab. 4).

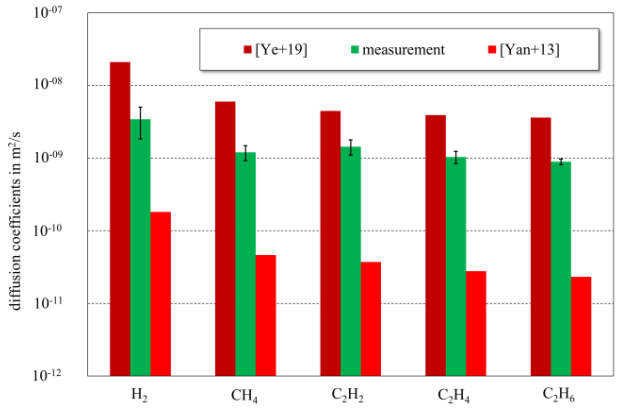

FIGURE 12. Measured diffusion coefficients compared with the literature.

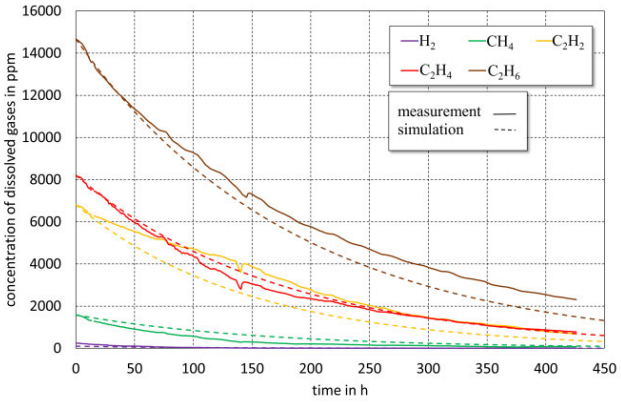

FIGURE 13. Comparison of simulation and measurement of gas losses for test vessel C at 25 °C.

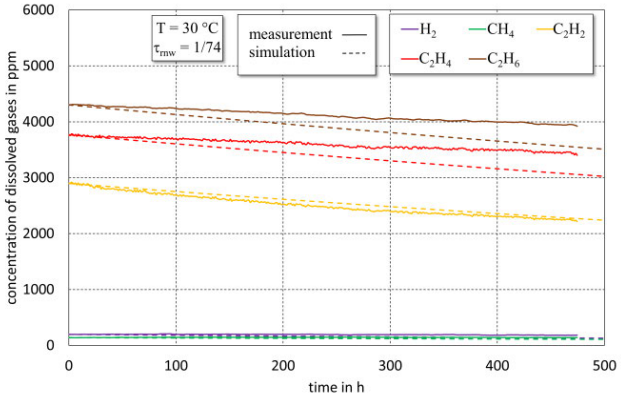

FIGURE 14. Measurement and simulation of the degassing of the distribution transformer at 30 °C with surface renewal theory.

It can be seen that – except for hydrogen – the results of the calculated Ostwald coefficients are in the same order of magnitude as those from the literature. The deviations can be attributed to different boundary conditions. The viscosity and composition of the mineral oil have a significant influence on the results [1]. In addition, any impurities in the samples have an influence.

Hydrogen proves to be a difficult gas to measure due to the small molecular sizes and consequently the great influence of the smallest impurities. Currently, science in general and CIGRE, in particular, are concerned with the measurement of solubilities and the associated problems [15].

2) DIFFUSION COEFFICIENTS

High concentrations of dissolved gas were used to determine the diffusion coefficients. In this concentration range, the mean cell factor is $\beta_{DC} = 1.04\ 1/cm^2$.

After every five test runs, the membrane was replaced. To prevent the loss of a time-consuming series of measurements due to contamination, two samples were taken from each concentration state and analysed several times. By this means it possible to quickly detect measurement errors. The measurements in which there were errors and strong deviations were not taken into account in the evaluation. Fig. 12 shows a comparison of the measured values with the literature.

F. CORRECTION OF GAS LOSSES

1) SIMPLE INTERFACES

In Fig. 13, the simulation with the developed model is compared with a measurement carried out in test object C, the geometry of which was also the basis for the simulation. The comparison shows good agreement between simulation and measurement for simple geometries. However, it should be noted at this point that the assumptions made here for the distances must be adapted for other test objects.

2) COMPLEX GEOMETRIES

In the surface renewal theory, a renewal time is based on the oil exchange and integrated into the calculation. In the considered case of the distribution transformer at $T_{oil} = 30$ °C, this results in a flow velocity of $u_{ex.} = 0.001$ m/s and thus an oil exchange time of around $\tau_{rnw} = 74$ h (Fig. 14).

It can thus be concluded that the theoretical model works in combination with an empirically determined exchange time constant. Without empirical measurements, it is not possible to determine the exchange time constant.

The time constant depends on the temperature and the geometry of the test specimen.

3) EFFECTS ON THE CONDITION ASSESSMENT

The developed model is used for free-breathing transformers and test setups by correcting the measured gas concentrations. Since it can happen in reality that a (continuous) measurement on a transformer is only installed later, a possible previous degassing must also be taken into account (Fig. 15).

It can be seen that the corrected values remain stable after a short-term defect and thus a falsification of the basis for interpretation is counteracted.

Fig. 16a shows the corresponding defect classification based on the measured original data. It is noticeable that the determined defect moves towards thermal defects with increasing degassing. If Fig. 16b is now compared with the

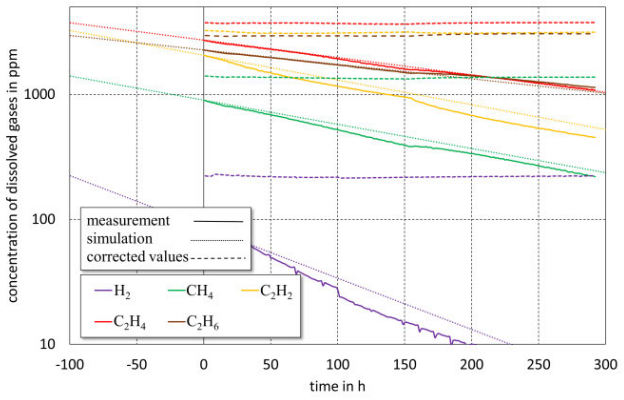

FIGURE 15. Measured values compared to the degassing simulated with the model and the values corrected with a retro-diction at the distribution transformer with 60 °C oil temperature.

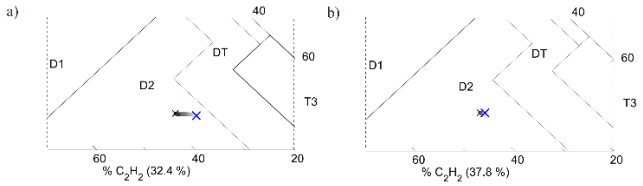

FIGURE 16. Defect classification with the duval triangle 1 (section) at the distribution transformer with 60 °C oil temperature.

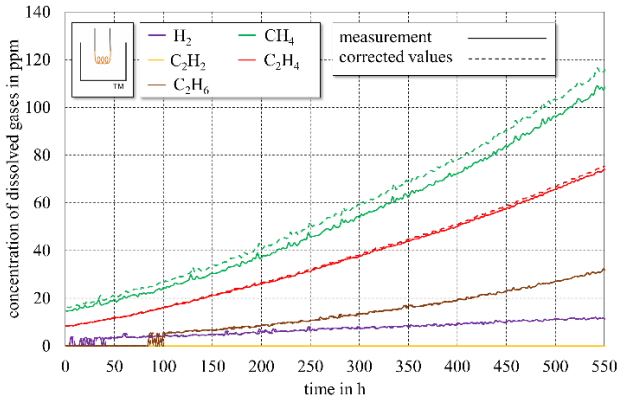

FIGURE 17. Original data and model adapted data of gas formation of a thermal fault-.

corrected values, it can be seen that the classification has largely stabilised.

Should there be a parallel gas formation due to an active defect, this is also taken into account (Fig. 17). Furthermore this means that the corrected rate of change can also be used for condition assessment. Depending on the concentration present and the initial detection of gases, the difference between the measured and corrected data varies.

V. CONCLUSION

With the measurements presented in this paper, it can be shown that the design – hermetically sealed or free-breathing – influences the condition assessment. The following findings were obtained/demonstrated:

- In the case of the free-breathing test objects, the gas losses could be demonstrated and quantified in combination with measurements on hermetically sealed arrangements.
- Another effect is that there is an equilibrium between gas production and gas losses. The gas losses are dependent on the concentration which leads to a specific equilibrium between the gas generation and the gas losses. This was proven in experiments. Consequently, this means that it can be confirmed that the condition can be misinterpreted by the gas losses in the case of both a continuous and a short-time defect.
- Furthermore, the experiments revealed that different gases degas at varying rates due to their chemical and physical properties (e.g. diffusion coefficients and molecular mobility). This leads to a shift in the relative ratios of different gases, which conventional methods, such as the Duval triangle method, do not take into account.
- Another aspect that was successfully demonstrated is that degassing depends on geometry and temperature. From the literature, an exponentially decreasing behaviour of the degassing time constant with increasing temperature and a linearly decreasing behaviour of the degassing time constant with the expansion of the interface were known and could be confirmed. Furthermore, the experiments showed an exponential relationship between the degassing time constants and the oil volume for simple geometries. For more complex geometric arrangements, other theories such as the surface renewal theory have to be added.

To further develop the condition assessment based on these findings, a principal model based on the general theories of mass transfer was developed and applied. It has been shown that this model and the resulting corrections to the concentration of dissolved gases can be used to calculate back to the true conditions. Thus, the falsification of the absolute gas concentrations on the one hand, as well as the shifting of the relative ratios on the other hand can both be counteracted.

Currently, some parameters of the model are still based on empirical measurements and therefore a general validity is not given. This means that the model must be adapted for each transformer through appropriate measurements. In further development steps, a purely mathematical determination of these parameters should lead to the comparatively simple creation of a digital twin. With its help, it should be possible to detect failures at an early stage.

REFERENCES

[1] C. Riedmann, U. Schichler, W. Häusler, and W. Neuhold, "Online dissolved gas analysis used for transformers—Possibilities, experiences, and limitations," *Elektrotechnik Informationstechnik*, vol. 139, no. 1, pp. 88–97, Feb. 2022, doi: 10.1007/s00502-022-00992-8.

[2] A. Müller, "Fehlergasverluste frei-atmender leistungstransformatoren," Ph.D. dissertation, Inst. Power Transmiss. High Voltage Technol., Univ. Stuttgart, Stuttgart, Germany, 2016.

[3] C. Riedmann and U. Schichler, "A physical model for the improvement of DGA-based condition assessment of power transformers," in *Proc. 8th Int. Conf. Condition Monit. Diagnosis (CMD)*, Phuket, Thailand, Oct. 2020, pp. 106–109.
[4] R. Anderson, U.-R. Roderick, V. Jaakkola, and N. Östman, "The transfer of fault gases in transformers and its effect upon the interpretation of gas analysis data," in *Proc. Int. Conf. Large High Voltage Electr. Syst.*, Paris, France, 1976.
[5] World Meteorological Organization. (Oct. 25, 2021). *WMO Greenhouse Gas Bulletin: The State of Greenhouse Gases in the Atmosphere Based on Global Observations Through 2020*. Accessed: Jan. 19, 2023. [Online]. Available: https://library.wmo.int/doc_num.php?explnum_id=10904
[6] E. K. Berner and R. A. Berner, *Global Environment: Water, Air, and Geochemical Cycles*, 2nd ed. Princeton, NJ, USA: Princeton Univ. Press, 2012.
[7] C. Riedmann and U. Schichler, "Online DGA—State of the art and influencing parameters," in *Proc. Int. Conf. Condition Monit. Diagnosis Maintenance (CMDM)*, Bucharest, Romania, 2019, pp. 250–257.
[8] H. Brauer, *Stoffaustausch Einschließlich Chemischer Reaktionen*. Frankfurt, Germany: Sauerländer, 1971.
[9] E. L. Cussler, *Diffusion: Mass Transfer in Fluid Systems*, 3rd ed. Cambridge, MA, USA: Cambridge Univ. Press, 2011.
[10] H. L. Toor and J. M. Marchello, "Film-penetration model for mass and heat transfer," *AIChE J.*, vol. 4, no. 1, pp. 97–101, Mar. 1958, doi: 10.1002/aic.690040118.
[11] R. Higbie, "The rate of absorption of a pure gas into a still liquid during short periods of exposure," *Trans. AIChE*, vol. 31, pp. 365–389, 1935.
[12] P. V. Danckwerts, "Significance of liquid-film coefficients in gas absorption," *Ind. Eng. Chem.*, vol. 43, no. 6, pp. 1460–1467, Jun. 1951, doi: 10.1021/ie50498a055.
[13] M. T. Imani, M. Farahani, M. Kuhnke, K. Homeier, and P. Werle, "Measuring methods for solubility of gases in insulation liquids," in *Proc. IEEE 19th Int. Conf. Dielectr. Liq. (ICDL)*, Manchester, U.K., Jun. 2017, pp. 1–4.
[14] *Standard Test Method for Estimation of Solubility of Gases in Petroleum Liquids*, ASTM Standard D 2779-92, 2020.
[15] S. Leivo, J. Larkio, P. Werle, and F. Scatiggio, "Determination of partition coefficients of gases for insulation liquids—Results of a CIGRE WG round Robin test," in *Proc. IEEE 21st Int. Conf. Dielectr. Liq. (ICDL)*, Seville, Spain, May 2022, pp. 1–4.
[16] *Oil-Filled Electrical Equipment—Sampling of Gases and Analysis of Free and Dissolved Gases—Guidance*, IEC Standard 60567, 2011.
[17] R. Sander, W. E. Acree, A. De Visscher, S. E. Schwartz, and T. J. Wallington, "Henry's law constants (IUPAC recommendations 2021)," *Pure Appl. Chem.*, vol. 94, no. 1, pp. 71–85, Dec. 2021, doi: 10.1515/pac-2020-0302.
[18] R. Battino, "The Ostwald coefficient of gas solubility," *Fluid Phase Equilibria*, vol. 15, no. 3, pp. 231–240, 1984, doi: 10.1016/0378-3812(84)87009-0.
[19] A. E. Baker, "Solubility of gases in transformer oil," in *Proc. 42nd Int. Conf. Double Clients*, Belmont, MA, USA, 1975.
[20] P. W. Atkins and J. de Paula, *Physical Chemistry*, 8th ed., New York, NY, USA: Freeman, 2006.
[21] *Standard Test Method for Solubility of Fixed Gases in Liquids (Withdrawn 2010)*, ASTM Standard D 2780-92, 2002.
[22] W. Ye, J. Hao, Y. Chen, M. Zhu, Z. Pan, and F. Hou, "Difference analysis of gas molecules diffusion behavior in natural ester and mineral oil based on molecular dynamic simulation," *Molecules*, vol. 24, no. 24, p. 4463, Dec. 2019, doi: 10.3390/molecules24244463.
[23] L. Yang, C. Qi, G. Wu, R. Liao, Q. Wang, C. Gong, and J. Gao, "Molecular dynamics simulation of diffusion behaviour of gas molecules within oil–paper insulation system," *Mol. Simul.*, vol. 39, no. 12, pp. 988–999, Oct. 2013, doi: 10.1080/08927022.2013.788180.
[24] J. H. Northrop and M. L. Anson, "A method for the determination of diffusion constants and the calculation of the radius and weight of the hemoglobin molecule," *J. Gen. Physiol.*, vol. 12, no. 4, pp. 543–554, Mar. 1929, doi: 10.1085/jgp.12.4.543.
[25] J. W. McBain and C. R. Dawson, "The diffusion of potassium chloride in aqueous solution," *Proc. Roy. Soc. London A, Math. Phys. Sci.*, vol. 148, no. 863, pp. 32–39, Jan. 1935, doi: 10.1098/rspa.1935.0003.
[26] A. R. Gordon, "The diaphragm cell method of measuring diffusion," *Ann. New York Acad. Sci.*, vol. 46, no. 5, pp. 285–308, Nov. 1945, doi: 10.1111/j.1749-6632.1945.tb36172.x.
[27] R. H. Stokes, "An improved diaphragm-cell for diffusion studies, and some tests of the method," *J. Amer. Chem. Soc.*, vol. 72, no. 2, pp. 763–767, Feb. 1950, doi: 10.1021/ja01158a032.
[28] T. Hashitani and R. Tamamushi, "Rapid measurements of diffusion coefficients of electrolytes in aqueous solutions by the diaphragm-cell method," *Trans. Faraday Soc.*, vol. 63, pp. 369–371, Aug. 1967, doi: 10.1039/tf9676300369.
[29] *IEEE Guide for the Interpretation of Gases Generated in Mineral Oil-Immersed Transformers*, IEEE Standard C57.104, 2019.

CHRISTOF RIEDMANN was born in Feldkirch, Vorarlberg, in 1990. He received the master's degree in electrical engineering and economics from the Graz University of Technology, in April 2017.

Since then, he has been a Scientific Project Assistant with the Institute of High Voltage Engineering and System Performance. He works in the field of condition assessment of electrical equipment, such as transformers, capacitors, generators, and overhead lines. He has extensive knowledge in the field of PD diagnostics and dissolved gas analysis.

UWE SCHICHLER (Member, IEEE) received the Ph.D. degree in electrical engineering from the Schering Institute, University of Hanover, in 1996.

He has been the Head of the Institute for High Voltage Engineering and Systems Performance, Graz University of Technology, since 2014. Then, he was with Siemens in the field of gas insulated switchgear and transmission lines. He has been an Austria's Representative in the CIGRE SC B3 "Switchgear," since 2014. He has participates in several CIGRE working groups. His current research interests include the condition assessment of electrical equipment, partial discharge measurements, cable technology, and DC insulation systems. He is a member of OVE, VDE, and CIGRE. He was received the "CIGRE Technical Award" of the D1 Study Committee.

WOLFGANG HÄUSLER was born in Graz, in 1964. He received the Graduate degree in communications engineering from HTL Bulme, Graz, in 1984.

He was a service and project technician in the field of process automation. Since 1990, he has been working independently in the field of measuring physical quantities, with a focus on humidity and temperature and gas compositions and has acquired a wealth of knowledge in his specializations.

WOLFGANG NEUHOLD was born in Graz, in 1963. He received the degree from BG Pestalozzi, Graz, in 1982.

Since 1997, he has been a Technical Employee with Ing. W. Häusler GmbH (IAG). During this time, he completed various technical and commercial training courses. He is currently the Product Manager of Moisture Meters, Gas Sensors, and Analyzers.